Solvent-Free Upcycling Vitrimers through Digital Light Processing-Based 3D Printing and Bond Exchange Reaction

Honggeng Li, Biao Zhang, Rong Wang, Xiaodan Yang, Xiangnan He, Haitao Ye, Jianxiang Cheng, Chao Yuan, Yuan-Fang Zhang, and Qi Ge*

Vitrimers, a type of dynamically crosslinked polymers that combine the solvent- and heat-resistance of thermosets with the reprocessability of thermoplastics, offer a new solution to the problem of plastic pollution. However, the current recycling approaches of vitrimers greatly constrain the shapes of recycled vitrimers to simple geometries, thus significantly limiting the application scopes of recycled vitrimers. Here, a simple but universal method for upcycling vitrimer wastes is reported by developing a UV curable recycling (UVR) solution system. Conventional unprintable vitrimer powders can be mixed with the UVR solution, and the resulting mixture is compatible with digital light processing based 3D printing to fabricate 3D structures with high resolution (up to 20 μm) and high geometric complexity. Heat treatment triggers bond exchange reactions in the printed structures, and greatly enhances the mechanical properties. This method allows to cyclically print vitrimer wastes multiple times. Moreover, the UVR-vitrimer mixture solution can work as an adhesive to bond printed small parts together to build a larger and more complex structure which cannot be printed. The upcycling method reported in this work extends the application scope of recycled vitrimers and provide a practical solution to address environmental challenges associated with plastic pollution.

1. Introduction

Vitrimers are a class of dynamically crosslinked polymers consisting of covalently adaptive networks (CANs) that can change their molecular topologies through thermally activated bond-exchange reactions (BERs).[1] The crosslinked networks endow vitrimers with the characteristics of thermosets, that is, high-temperature mechanical, thermal, and environmental resistance,[2] while CANs impart the reprocessability of thermoplastics to the chemically crosslinked vitrimers.[2b,3] Despite a variety of vitrimers having been developed,[2b,4] the methods for recycling vitrimers are constrained to injection molding,[2b] hot pressing,[5] welding,[6] and solvent-assisted recycling,[7] which greatly limit the geometric complexity and precision of reprocessed vitrimer structures (**Figure 1**a).

3D printing that creates complex 3D objects in a layer-by-layer fashion has shown great potentials in reprocessing vitrimers to complex 3D geometries. Shi et al. proposed a method that uses direct ink writing-based 3D printing to cyclically 3D print epoxy-acid vitrimer into different 3D structures.[8] However, the manner of printing 3D structures by extruding vitrimer ink limits the printing resolution and geometric complexity.[9] More importantly, this method requires substantial addition of recycling solvent, for example, ethylene glycol, to depolymerize the printed structures. To complete a cycle of reprocessing 3D-printed epoxy-acid vitrimers, the recycling solvent needs to be evaporated, which leads to unnecessary waste and potential risk of safety. Recently, Zhang et al. developed a type of 3D printable vitrimer, that is, a 3D printing reprocessable thermosetting material (3DPRT), which is not only ultraviolet (UV) curable thus compatible with digital light processing (DLP)-based high-resolution 3D printing, but also reprocessable, that is, reshapable, repairable, and recyclable, through BERs.[4f] However, in this work, the recycling approach was limited to hot pressing, and cyclically printing of 3DPRT was not realized.

Here, we report a solvent-free method to upcycle vitrimers so that the conventional unprintable vitrimers can be reprocessed through DLP-based 3D printing to fabricate vitrimer 3D structure with complex geometry and high resolution. As

H. Li, R. Wang, X. Yang, X. He, H. Ye, J. Cheng, Q. Ge
Department of Mechanical and Energy Engineering
Southern University of Science and Technology
Shenzhen 518055, China
E-mail: geq@sustech.edu.cn

B. Zhang
Frontiers Science Center for Flexible Electronics (FSCFE)
Xi'an Institute of Flexible Electronics (IFE) and Xi'an Institute
of Biomedical Materials & Engineering (IBME)
Northwestern Polytechnical University
127 West Youyi Road, Xi'an 710072, China

C. Yuan
State Key Laboratory for Strength and Vibration
of Mechanical Structures
Department of Engineering Mechanics
Xi'an Jiaotong University
Xi'an 710049, China

Y.-F. Zhang
Digital Manufacturing and Design Centre
Singapore University of Technology and Design
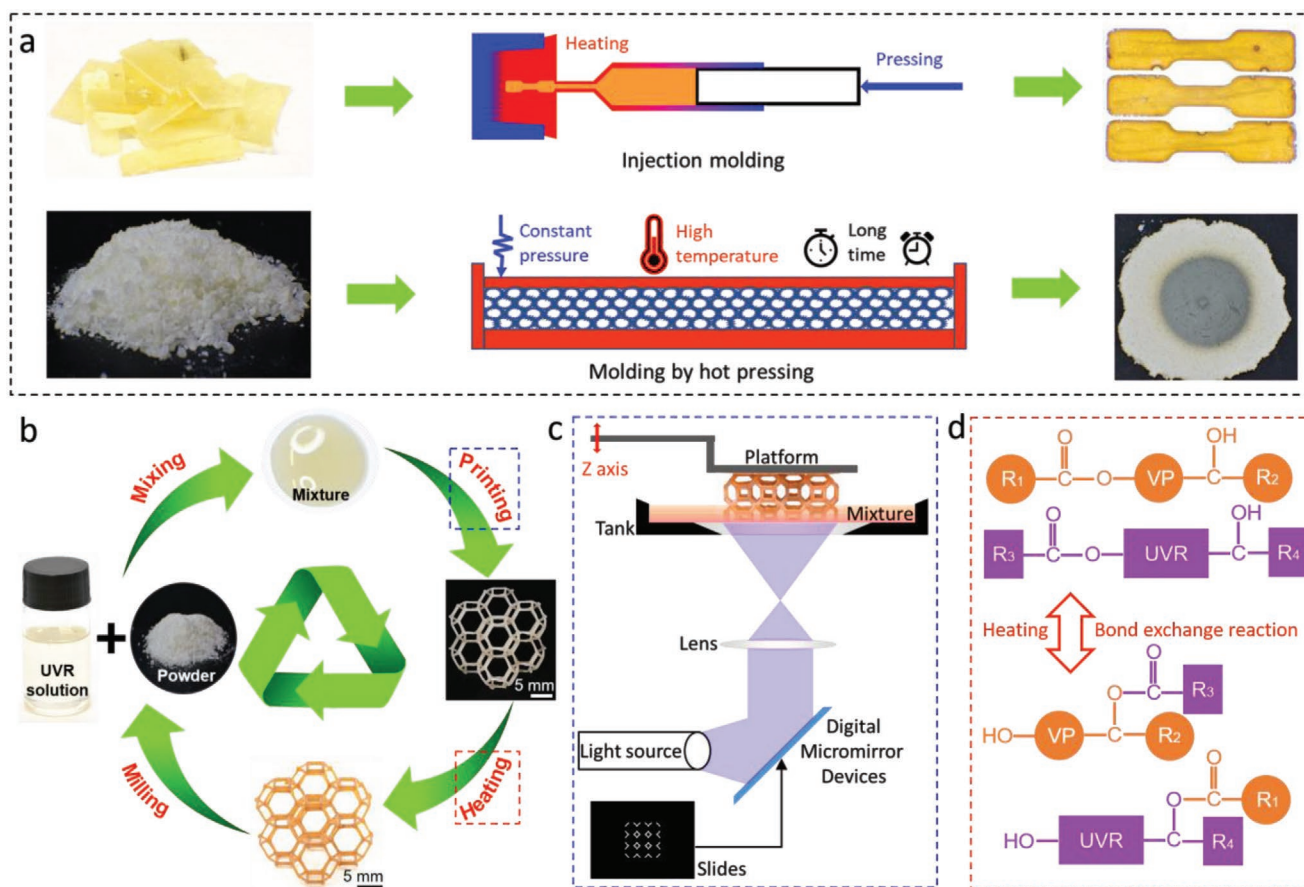Singapore 487372, Singapore

Figure 1. Recycling vitrimers through DLP-based 3D printing and bond exchange reaction. a) Illustration of traditional methods used to recycle vitrimers. b) Illustration of a full cycle that reprocesses vitrimers into complex 3D geometry through DLP-based 3D printing and BERs. c) Schematic illustration of DLP-based 3D printing. d) The bond exchange reaction promotes the interfacial fusion of UVR and vitrimer powders during the heat treatment. VP, vitrimer powders; UVR, UV-curable recycling resin; R_1, R_2, R_3, and R_4, the possible middle chains in acrylate polymer.

shown in Figure 1b, we started the process of recycling a vitrimer by grinding it into microparticle powders. Then, a UV curable mixture precursor solution was prepared by mixing the vitrimer powders into a UV-curable recycling (UVR) solution consisting of acrylate functional group for photopolymerization during DLP-based 3D printing, and hydroxy as well as ester functional groups for transesterification-based BERs. As illustrated in Figure 1c, the UV curable mixture precursor solution loaded with vitrimer powders is compatible with DLP-based 3D printing system to print 3D structures with complex geometry and high resolution. Finally, as shown in Figure 1d, heat treatment was applied to trigger the BERs between vitrimer powders and 3D networks resulted from photopolymerization of UVR solution, which makes the two materials covalently bonded and emerge into a material. The printed vitrimer structures can be further recycled by milling it to powders, and then mixing the vitrimer powders with the UVR solution again. Compared with previous recycling methods, the method proposed in this work upgrades the recycled vitrimers in terms of structure, property, function, and application (Figure S1, Supporting Information), and is solvent-free thus more eco-friendly and safer (Figure S1 and Table S1, Supporting Information). The proposed method is more general, and can be applied to recycle epoxy-anhydride

hard vitrimer,[5e] epoxy-acid soft vitrimer,[5d] and other transesterification-based vitrimers.[4c,d,5d,10] It is even possible to recycle other types of vitrimers by following the same design for UVR solution but replacing the transesterification-related functional groups with other dynamic covalent groups such as borate ester exchange,[4e] transcarbamoylation,[4b] and transalkylation.[11] More importantly, as the materials printed with UVR solution are also vitrimers, the developed UVR solution can be used to recycle the structures printed with UVR solution itself. Therefore, a fully cyclical DLP-based 3D printing can be realized through the method proposed in this work.

2. Results and Discussion

Figure 2 describes the chemical details on upcycling vitrimers. UVR solution plays a key role in recycling the transesterification-based vitrimers. We design the UVR solution through a two-step polymerization strategy. Figure 2a presents the possible chemicals for preparing a UVR solution. The monomer has mono-functional acrylate group for building linear chains during 3D printing, and the crosslinker has di-functional acrylate group for crosslinking the linear chains to form
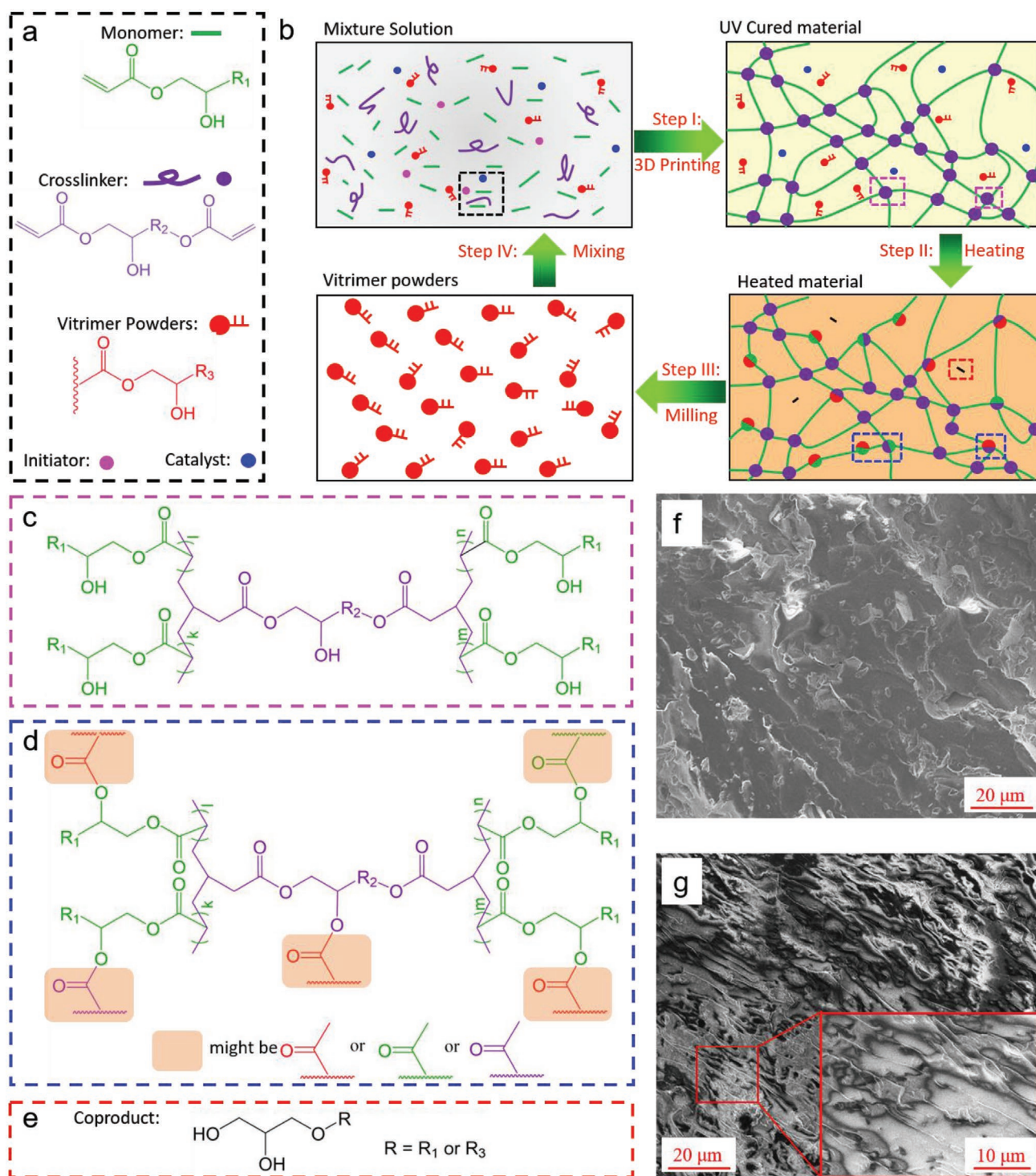
ADVANCED
SCIENCE NEWS
www.advancedsciencenews.com

ADVANCED
FUNCTIONAL
MATERIALS
www.afm-journal.de

Figure 2. Materials and upcycling mechanism. a) Chemicals for each part of UVR solution. b) Illustration shows the 3D printing and heat treatment process for recycling vitrimer. Purple dots: permanent covalent bonds; two-color dots: dynamic covalent bonds. c) The covalently crosslinked networks formed by the double bonds on the acrylate functional groups on both monomer and crosslinker of the UVR solution. d) The bond exchange reactions between the hydroxy and ester functional groups on both 3D printed polymer networks and vitrimer powders. e) Coproduct of bond exchange reaction. f) The SEM image of fracture surface of as-printed sample (no heat treatment after printing). g) The SEM images of fracture surface of heat-treated sample. R1, R2, and R3: the possible middle chains in acrylate polymer.

polymer networks during 3D printing. More importantly, both monomer and crosslinker have ester and hydroxyl functional groups that are involved in the transesterification-based BERs during heating treatment. In addition, photoinitiator should be

**ADVANCED
SCIENCE NEWS**
www.advancedsciencenews.com

**ADVANCED
FUNCTIONAL
MATERIALS**
www.afm-journal.de

Table 1. Monomers for UVR solution.

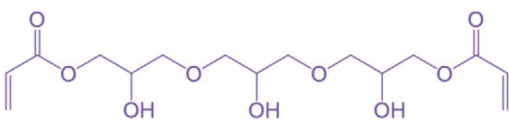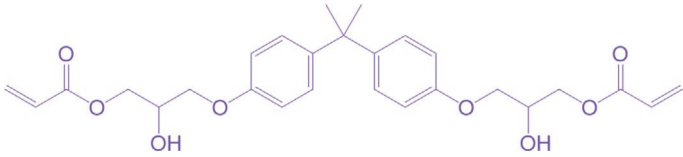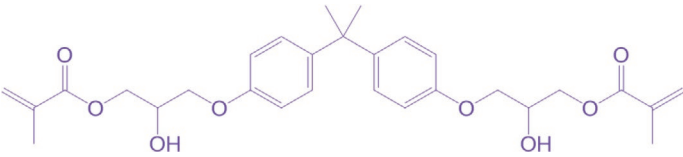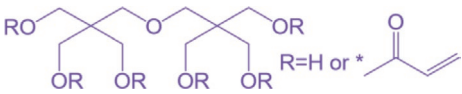| Monomers for UVR	Chemical structure	Molecular weight [g mol⁻¹]
2-Hydroxyethyl acrylate		116.12
4-Hydroxybutyl acrylate		144.17
Hydroxypropyl acrylate, mixture of isomers		130.14
Poly(ethylene glycol) methacrylate		360/500
2-Hydroxy-3-phenoxypropyl acrylate		222.24
3-Chloro-2-hydroxypropyl methacrylate		178.61
Hydroxybutyl methacrylate, mixture of isomers	R=(1:1) H or	158.19
2-Hydroxyethyl methacrylate		130.14
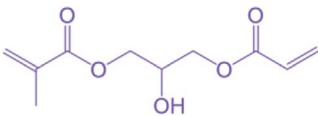
added to the UVR solution for initiating photopolymerization during DLP-based 3D printing, and a metal catalyst needs to be added to accelerate BERs. **Tables 1** and **2** present the possible monomers and crosslinkers for preparing UVR solutions. We chose seven combinations of monomer and crosslinker to prepare seven different UVR solutions (**Table 3**). Figure S2, Supporting Information, shows that the heating treatment raises the moduli of the samples prepared with seven UVR solutions by 20 to 100 times resulted from the heating triggered BERs (details of UVR solution synthesis are in Experimental Section). In this work, we prepared the UVR solution by using 2-hydroxy-3-phenoxypropyl acrylate as monomer and bisphenol A glycerolate (1 glycerol/phenol) diacrylate as crosslinker as it (UVR-7 in Table 3) reaches the highest modulus (900 MPa) after the heating treatment. Details on preparation of the UVR solution can be found in Experimental Section. Figure 2a also shows the possible chemical structure of the to-be-recycled vitrimer which has ester and hydroxyl functional groups for transesterification-based BERs. The unprintable vitrimers used for the upcycling experiments are epoxy-anhydride vitrimer[2b] (referred to as "hard vitrimer" here due to its high modulus) and epoxy-acid vitrimer[2b] (referred to as "soft vitrimer" here due to its low modulus). Details on preparation of hard

vitrimer and soft vitrimer can be found in Figure S3, Supporting Information.

Figure 2b illustrates a full cycle that upcycles vitrimer through DLP-based 3D printing and BER. In Step I—3D printing, localized UV curing from a DLP-based 3D printer converts liquid mixture precursor solution consisting of the UVR solution loaded with vitrimer powders into solid 3D structure. UV irradiation excites the photoinitiator to generate free radicals which open the double bonds on the acrylate functional groups on both monomer and crosslinker of the UVR solution to form covalently crosslinked networks (detailed chemical structure can be seen in Figure 2c). It should be noted that after 3D printing, the vitrimer molecules are physically surrounded by the polymer networks resulted from photopolymerization of the UVR solution, but they are not chemically bonded. In Step II, the heating treatment activates the transesterification-based BERs between the hydroxy and ester functional groups on both 3D printed polymer networks and vitrimer powders, which covalently integrates the vitrimer molecules into the 3D printed polymer networks (possible chemical structures are shown in Figure 2d), and further enhances mechanical performance of printed structure. In addition, the heating-triggered BERs may generate some small molecules which have two hydroxyl groups on one molecule (Figure 2e). Once the upcycled vitrimer structure needs to be recycled one more time, we can grind the structure into powders (Step III), and then mix the powders into the UVR solution to prepare the UVR–vitrimer mixture precursor solution again for the next round of vitrimer recycling (Step IV). We applied scanning electron microscopy (SEM) to investigate the fracture surfaces of the as-printed sample (no heat treatment after printing) and heat-treated sample (details can be found in Experimental Section). As shown in Figure 2f, the uniformly distributed vitrimer powder particles can be clearly observed on the fracture surface of the as-printed sample. The heat treatment triggers BERs between the vitrimer particles and the matrix made of UVR, which leads to the merge between the two parts. Therefore, we could not see obvious vitrimer powder particles but a smooth surface on the fracture surface of the heat-treated sample (Figure 2g).

Preparing the mixture precursor solution consisting of UVR solution loaded with vitrimer powders (details can be found in Experimental Section, Materials) is the key step in upcycling vitrimer through DLP-based 3D printing and BERs. Therefore, it is critical to investigate the relevant properties of the vitrimer powders and the mixture precursor solutions. We ground both hard and soft vitrimer samples into powders using a commercial milling machine (details can be found in Experimental Section). We performed SEM to investigate morphology of both hard and soft vitrimer powders (SVP) (details can be found in Experimental Section). As shown in **Figure 3**a, the particle sizes of the most powders are less than 20 μm. Figure 3b presents the particle size distribution analyzed by a laser granularity apparatus (details can be found in Experimental Section). The particle size distributions of both soft and hard vitrimer powders follow the same trend, and the diameters of more than 90% particles are less than 18 μm. The above characterizations suggest that the particle sizes of the vitrimer powders are relatively small, which makes the UVR–vitrimer mixture precursor solutions suitable for DLP-based 3D printing.

**ADVANCED
SCIENCE NEWS**
www.advancedsciencenews.com

**ADVANCED
FUNCTIONAL
MATERIALS**
www.afm-journal.de

Table 2. Crosslinkers for UVR solution.

Crosslinkers for UVR	Chemical structure	Molecular weight [g mol⁻¹]
3-(Acryloyloxy)-2-hydroxypropyl methacrylate		214.22
Glycerol 1,3-diglycerolate diacrylate		348.35
Bisphenol A glycerolate (1 glycerol/phenol) diacrylate		484.54
Bisphenol A glycerolate dimethacrylate		512.59
Dipentaerythritol penta-/hexa-acrylate	R=H or *	524.51

Viscosity is one of the key properties that determine whether the precursor solution is suitable for DLP-based 3D printing. Thus, we preformed rheological tests to investigate the effect of vitrimer powder content on viscosity of the mixture precursor solutions. Detailed information on rheological tests can be found in Experimental Section. As shown in Figure 3c, the increase in the content of hard vitrimer powders (HVP) leads to the rise in mixture solution's viscosity. When the HVP content is not more than 25 wt%, the mixture solution is Newtonian fluid, and the viscosity is less than 4 Pa·s. When the HVP content is more than 25 wt%, the shear thinning effect can be observed, but the viscosity is much greater than that of the solution suitable for DLP-based 3D printing.[12] Figure 3d

presents the effect of the SVP content on the viscosity of the mixture precursor solution, which is almost identical with Figure 3c. Therefore, we prepared the mixture precursor solutions with 25 wt% vitrimer powders to ensure that the mixture precursor solutions have sufficient fluidity for DLP-based 3D printing. In addition, as shown in Figure S4, Supporting Information, the prepared mixture precursor solutions are stable, and no apparent precipitations were observed after being stored at room temperature for 1 month in a dark environment.

UV curing time is another key property that determines whether the precursor solution is suitable for DLP-based 3D printing. As shown in Figure 3e, the pure UVR solution exhibits excellent photo-activity: UV curing a 200 µm thick layer with UV light intensity of 1 mW cm⁻² only takes 5 s, and the UV curing time can be further decreased to 1 s by increasing the UV light intensity to 8 mW cm⁻². Mixing 25 wt% vitrimer particles to UVR solution slightly weakens the photo-activity, but UV curing a 200 µm thick layer with a UV light intensity of 1 mW cm⁻² only requires 9 s, which confirms that the mixture precursor solution is still suitable for DLP-based 3D printing. In addition, as shown in Figure S5, Supporting Information, the curing depth decreases after adding more vitrimer particles.

The vitrimer particles in the mixture precursor solution affect the resolution of printed structures. We printed planar grids with different widths (10, 20, and 40 µm) to investigate this effect. As shown in Figure 3f, when the grid width is 10 µm, it can be seen that some giant particles with greater size (≈20 in diameter) are embedded in the grid rods, which leads to the unsmooth and discontinuous grid rods. When the grid width increases to the scales (20 µm and 40 µm) comparable with the size of those giant particles, the smoothness and continuity of

Table 3. Selected monomer and crosslinker combinations in UVR series formulations.

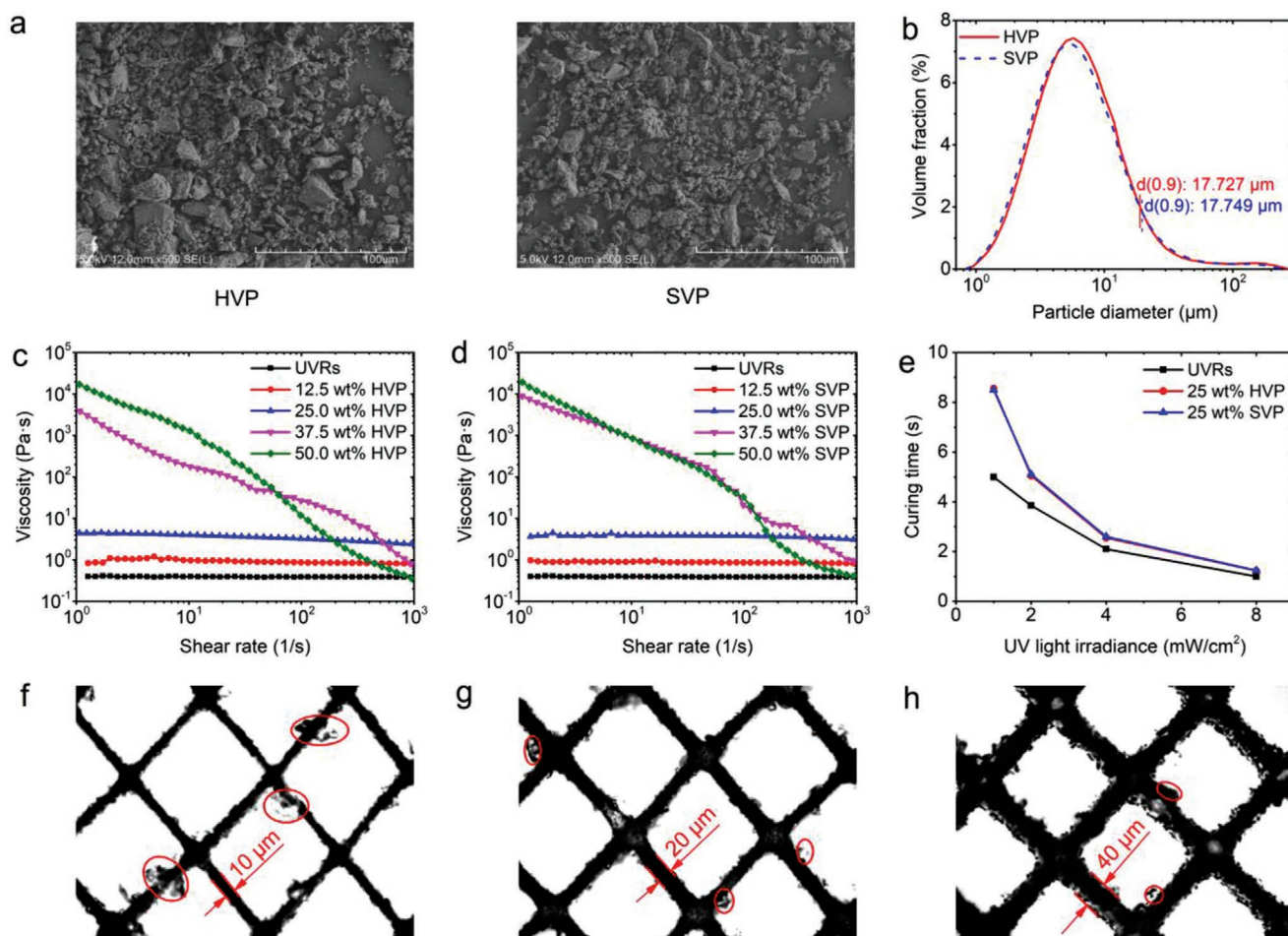| UVR series	Monomer	Crosslinker
UVR-1	2-Hydroxyethyl acrylate	3-(Acryloyloxy)-2-hydroxypropyl methacrylate
UVR-2	2-Hydroxyethyl acrylate	Glycerol 1,3-diglycerolate diacrylate
UVR-3	4-Hydroxybutyl acrylate	3-(Acryloyloxy)-2-hydroxypropyl methacrylate
UVR-4	4-Hydroxybutyl acrylate	Glycerol 1,3-diglycerolate diacrylate
UVR-5	Hydroxypropyl acrylate (mixture of isomers)	3-(Acryloyloxy)-2-hydroxypropyl methacrylate
UVR-6	Hydroxypropyl acrylate (mixture of isomers)	Glycerol 1,3-diglycerolate diacrylate
UVR-7	2-Hydroxy-3-phenoxypropyl acrylate	Bisphenol A glycerolate (1 glycerol/phenol) diacrylate

Figure 3. Characterization of vitrimer powders and UVR–vitrimer mixture solution. a) SEM images of HVP and SVP. b) Particle size distribution of HVP and SVP measured by laser particle size analyzer. c,d) Viscosities of UVR solution and UVR–vitrimer mixture solutions. e) Gel times of UVR solution and UVR–vitrimer mixture solutions with 25 wt% vitrimer powders. f–h) Effect of powder on printing accuracy (printed by UVR–vitrimer mixture solution with 25 wt% HVP): f) 10 μm grid, g) 20 μm grid, h) 40 μm grid. HVP, hard vitrimer powders; SVP, soft vitrimer powders.

grid rods are greatly improved (Figure 3g,h). However, even for the 40 μm grids, the slightly rough surface still can be observed due to the existence of the small vitrimer powders.

During the process of upcycling vitrimers, the heating treatment applied to the 3D printed structures triggers the transesterification-based BERs which bond the polymer networks made of UVR solution covalently with vitrimer particles, and stiffen the printed structures. To study the effect of heating treatment on the mechanical properties of upcycled vitrimers, we conducted dynamic mechanical analysis (DMA) and uniaxial tensile tests with samples that were thermally treated at 180 °C for 0, 1, 2, 3, 4, 6, and 8 h, respectively. **Figure 4**a,b shows the storage modulus and tan δ versus temperature for the samples made of UVR–vitrimer mixture solution with 25 wt% hard vitrimer powders (25 wt% HVP), where the storage modulus describes the elastic response of the material and the peak of tan δ indicates the glass transition temperature (T_g).[13] The increase in the heating treatment time from 0 to 8 h results in a gradual increase in the rubbery modulus (the lower modulus plateau at high temperatures) from ≈6 to ≈11 MPa (Figure 4a), which suggests an increase in dynamic crosslinking points

during BERs. Moreover, as shown in Figure 4b, the increase in dynamic crosslinking points does not only raises the rubbery modulus but also shifts the peak of tan δ to a higher temperature as the generation of additional crosslinks restricts segmental chain mobility, and therefore leads to higher T_g.[4f] Figure 4c presents the room-temperature uniaxial tensile testing results for the recycled samples with 25 wt% HVP. The longer heating treatment also makes the recycled sample have higher Young's modulus which increases from ≈40 to ≈1000 MPa.

Figure 4d–f shows the DMA and uniaxial tensile testing results for the samples made of the UVR–vitrimer mixture solution with 25 wt% SVP under different heating durations. Similar to Figure 4a–c, the longer heating treatment leads to higher rubbery modulus, higher T_g, as well as higher room-temperature Young's modulus. Interestingly, the heating treatment leads to two peaks on the tan δ, which can be attributed to the large different thermomechanical properties between the soft vitrimer and the pure material made of UVR solution especially in rubbery modulus and T_g (Figure S6, Supporting Information).[5c]

Since the materials printed with UVR solution are also vitrimers, the UVR solution can be used to recycle the structures
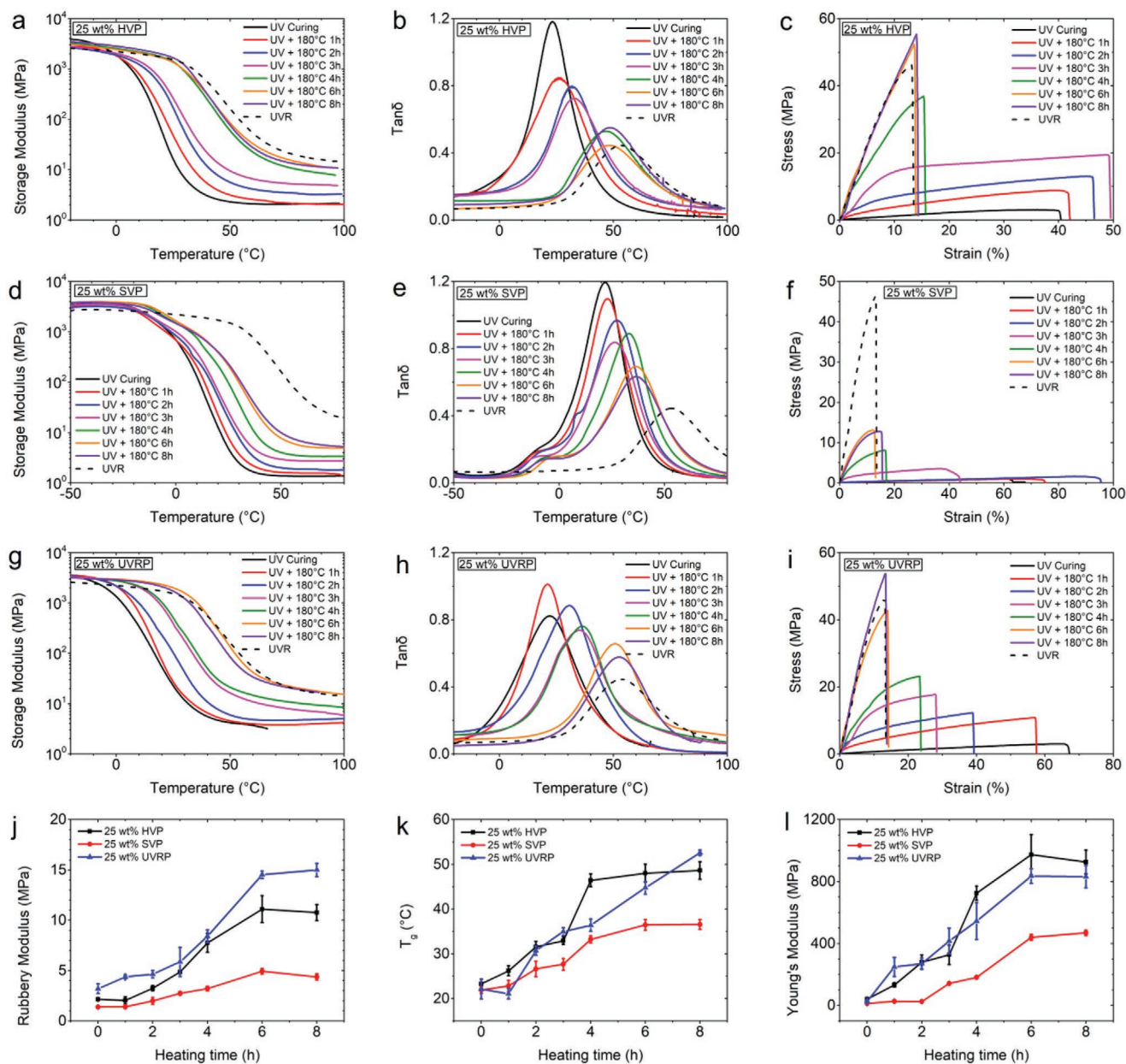
**ADVANCED
SCIENCE NEWS**

www.advancedsciencenews.com

**ADVANCED
FUNCTIONAL
MATERIALS**

www.afm-journal.de

Figure 4. Thermomechanical and mechanical properties of the mixtures for DLP 3D Printing. a–c) Storage modulus, tanδ, and stress–strain behavior of cured 25 wt% HVP with different heating times. d–f) Storage modulus, tanδ, and stress–strain behavior of cured 25 wt% SVP with different heating times. g–i) Storage modulus, tanδ, and stress–strain behavior of cured 25 wt% UVRP with different heating times. j) Effect of heating time on the rubbery modulus. k) Effect of heating time on the glass transition temperature (T_g). l) Effect of heating time on the Young's modulus. 25 wt% HVP: UVR–hard vitrimer mixture solution with 25 wt% hard vitrimer powders. 25 wt% SVP: UVR–soft vitrimer mixture solution with 25 wt% soft vitrimer powders. 25 wt% UVRP: UVR–UVR powder mixture solution with 25 wt% UVR powders.

printed with UVR itself. Therefore, we also carried out DMA and uniaxial tensile tests to investigate the effect of heating duration on the thermomechanical performance of the samples made of UVR–UVR particle solution with 25 wt% UVR powders (25 wt% UVRP). As shown in Figure 4g–i, the increase in heating duration leads to higher rubbery modulus, T_g, and room-temperature Young's modulus until the number of dynamic crosslinking points reaches equilibrium.

The effects of heating time on these three key thermomechanical properties are also summarized in Figure 4j–l. After

the 6 h thermal treatment, the dynamic crosslinking points reach a dynamic equilibrium beyond which no apparent increase in rubbery modulus, T_g, and Young's modulus are observed.

The proposed method enables upcycling vitrimers multiple times. As demonstrated in **Figure 5**a, a vitrimer waste was recycled to prepare the UVR–vitrimer mixture solution which was used to print buckliball. In the second round of upcycling, the buckliball was crushed and ground into vitrimer powders to prepare the UVR–vitrimer mixture solution, which could be
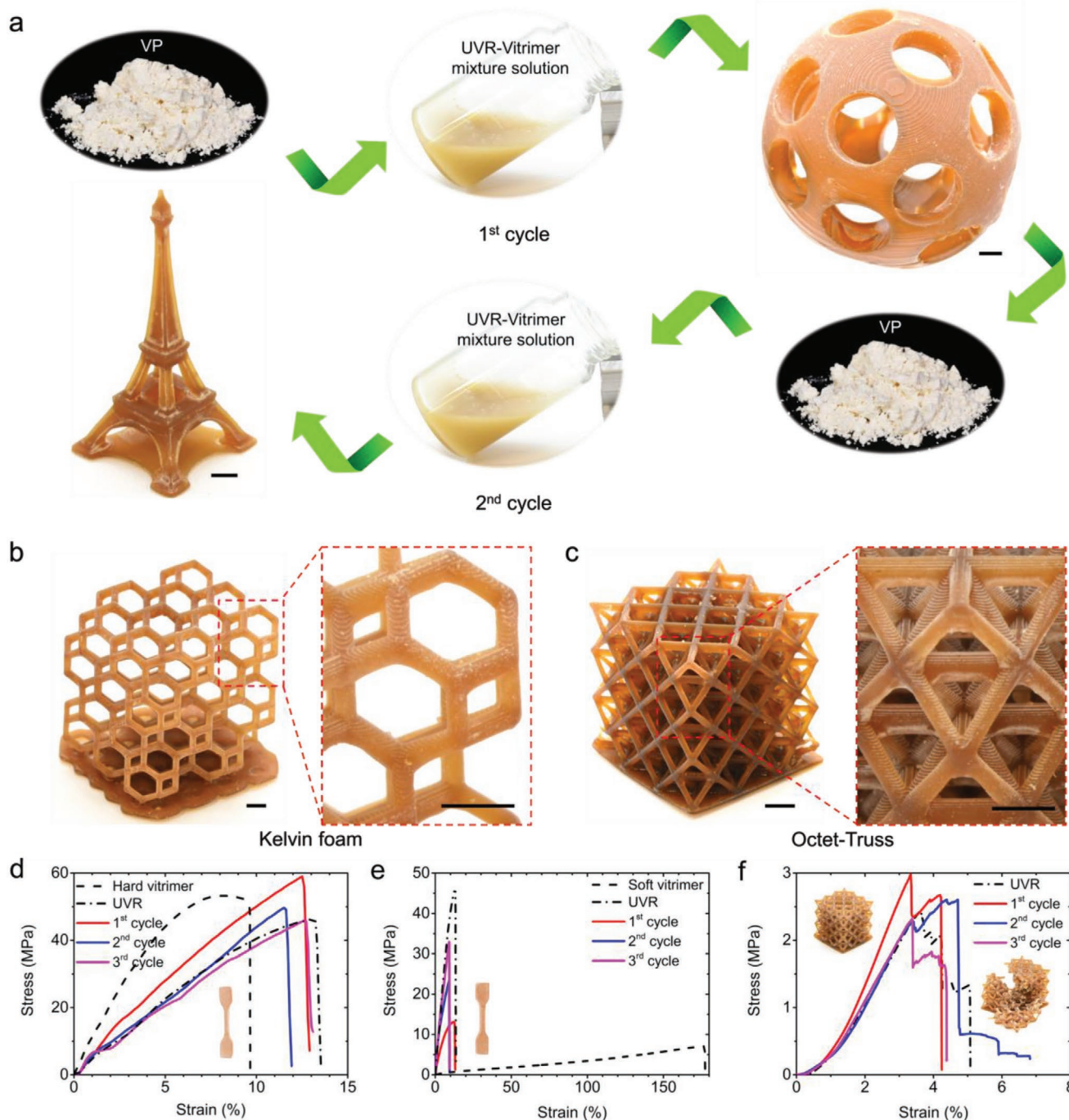
Figure 5. Multiple upcycles of vitrimers with high-precision and high complexity manufactured through DLP 3D printing and bond exchange reaction. a) Flow chart of twice upcycling vitrimer. b,c) Upcycled vitrimer structures with high resolution and high complexity (b, Kelvin foam; c, octet-truss). d,e) Uniaxial tensile tests to examine the mechanical repeatability of the recycled UVR–vitrimer mixture solution (d, UVR–hard vitrimer mixture; e, UVR–soft vitrimer mixture). f) Quasi-static compression test to examine the mechanical repeatability of octet-truss for upcycled UVR–hard vitrimer mixture. Scale bar: 2 mm.

used to print a new 3D structure such as an Eiffel Tower. With DLP-based 3D printing, bulk vitrimer wastes can be upcycled to produce high-resolution and complex 3D structures. As shown in Figure 5b, c, the UVR–vitrimer mixture solution can be used to print highly complex lattice structures, such as Kelvin form and octet-truss, respectively.

We also carried out uniaxial tensile tests to investigate the mechanical properties of the UVR–vitrimer samples which were recycled multiple times. As presented in Figure 5d,e, the mechanical properties of the recycled UVR–vitrimer samples tend to be similar to that of the sample made of pure UVR due to the continuous addition of UVR solutions in each cycle.
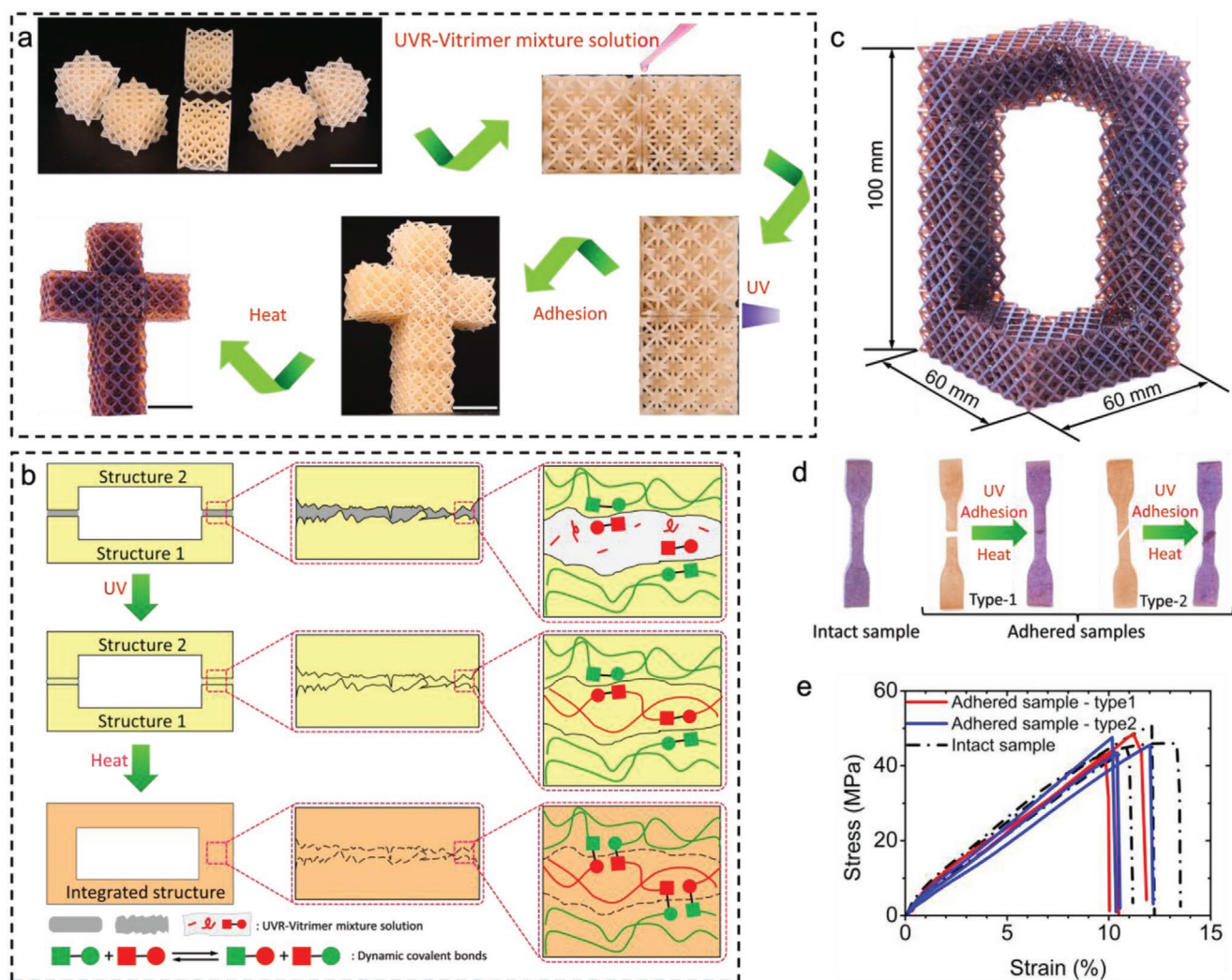
Figure 6. Unsupported large-scale, high-precision 3D components are realized through UV curing adhering and thermally induced bond exchange reaction. a) Adhesion process of multiple octet-truss structures (scale bar: 20 mm). b) Illustration of the details of the adhesion process. c) Realizing a large-scale, high-precision, high-complexity 3D model of unsupported structure through the adhesion method. d) Snapshots of the intact sample and adhered samples. e) The effect of adhesion interface on the mechanical properties of materials.

As shown in Figure 5d, the modulus of the pure hard vitrimer sample is 1340 MPa, which is close to that of the pure UVR sample (≈900 MPa). Therefore, it is observed that after two cycles of recycling, the modulus of the recycled sample equilibrates at 900 MPa. In Figure 5e, due to the significant difference in mechanical property between the soft vitrimer and the UVR material, the stiffness of recycled vitrimer is gradually increased from 430 MPa (after 1st cycle) to 981 MPa (after 3rd cycle). Of course, one can adapt the moduli of the recycled vitrimers to lower values by choosing the UVR solution recommended in Table 3 and Figure S2, Supporting Information, with lower modulus. In addition, we further investigated the variations in mechanical property of 3D printed structures by compressing the printed octet-truss structures resulted from different recycling cycles. As presented in Figure 5f, the results of quasi-static compression experiments show that the mechanical property of the octet-truss structures printed with the UVR–vitrimer mixture solution with hard vitrimer particles are

close to that of the octet-truss structure printed with pure UVR solution. Therefore, this approach enables upcycling vitrimers into complex 3D structures without sacrificing mechanical properties.

The prepared UVR–vitrimer mixture solution enables not only direct printing 3D structure, but also bonding individually printed parts to build a structure which might be larger than the volume that a commercial desktop DLP 3D printing can cover, or too complex to be directly printed. As demonstrated in **Figure 6**a, we printed several octet-truss lattice structures made of UVR–vitrimer mixture solution consisting of 25 wt% hard vitrimer particles, and adhered them together by generating an adhesive layer between them. The adhesive layer was formed by UV curing the UVR–vitrimer mixture solution, which was deposited into the gap between the two structures. Following this procedure, we made a cross shape consisting of six octet-truss lattice structures. Finally, we enhanced the mechanical performance of the whole cross shape structure

through heating treatment. Figure 6b illustrates the details during the adhesion process. The UVR–vitrimer mixture solution fills the voids created between the microscopically rough surfaces of the two structures. After UV curing, the UVR solution solidifies, but the solidified UVR is not covalently bonded with the printed structures. The heating treatment triggers BERs that penetrate the boundaries between the solidified UVR and the two printed structures, so that the three parts are covalently bonded together. Compared with the hot pressing method for welding vitrimers,[5b,6a] using the UVR solution as adhesive does not need to apply force during the heating treatment to hold the two vitrimer parts together, and therefore, would not cause unwanted deformation of the welding site. This adhesion approach also allows us to create structures which are difficult to be directly printed. Figure 6c presents a relatively larger overhang structure which was created by adhering 16 octet-truss unit structures but could not be directly 3D printed without using supporting parts. As shown in Figure 6d, we further compare the mechanical performance of the intact dumbbell sample ("intact sample" for short) with that of the sample made by adhering the two identical half parts through BERs ("adhered sample" for short). Both samples were fabricated by using the UVR–vitrimer mixture solution with 25 wt% of hard vitrimer particles. For the adhered samples, we also designed two types of adhesion interface: 1) The interface is normal to the length direction; 2) the interface is at a 45° incline to the length direction. The comparison in Figure 6e shows that the adhered sample behaves nearly the same as the intact sample; the adhered samples with different interface types exhibit nearly the same stress–strain behavior. More importantly, the fact that the fracture interface of the adhered sample is not along the adhesion interface indicates the proposed adhesion approach imparts the adhered sample a robust adhesion interface (Figure S7, Supporting Information).

3. Conclusion

In summary, we developed a simple and universal method to upcycle vitrimer wastes by developing a UVR solution system. Conventional unprintable vitrimers powders can be mixed with the UVR solution, and the resulting mixture is compatible with DLP-based 3D printing to fabricate 3D structures with high resolution (up to 20 μm) and high geometric complexity. Heat treatment triggers bond exchange reactions in the printed structures, and greatly enhances the mechanical properties. This method allows us to cyclically print vitrimer wastes multiple times. Moreover, the UVR–vitrimer mixture solution can work as an adhesive to bond printed small parts together to build a larger and more complex structure which could not be printed. Although the study in this paper is limited to transesterification-based vitrimers, it is expected that this upcycling technology through 3D printing and BERs can be further extended to other dynamic covalent chemicals. Therefore, the upcycling method reported in this work extends the application scope of recycled vitrimers, and provides a practical solution to address environmental challenges associated with plastic pollution.

4. Experimental Section

UVR Solution: In the UVR solution used in this paper, the weight ratio of monomer (2-hydroxy-3-phenoxypropyl acrylate) and crosslinker (bisphenol A glycerolate (1 glycerol/phenol) diacrylate) was 9:1. The concentration of catalyst (zinc acetylacetone hydrate, $Zn(acac)_2$) was 5 mol% to the OH groups. The amount of the initiator (diphenyl(2,4,6-trimethylbenzoyl) phosphine oxide) was 2 wt% of the total weight of monomer and crosslinker. All chemicals were purchased from Sigma–Aldrich and used as received. The catalyst was first added in monomer and dissolved at around 70 °C. Then, the initiator was added and mixed at room temperature. Finally, the crosslinker was added into the system.

Vitrimer Powders: First, bulk samples were ground into powders by using Variable Speed Rotor Mill PULVERISETTE 14 (FRITSCH, Germany) with a 0.5 mm trapezoidal perforation sieve ring. Then, the above powder was ground with a miniature omnidirectional planetary ball mill machine (F-P400E, FOCUCY, China) for 8 h. Zirconia ceramic grinding balls with diameters of 2, 5, and 10 mm were placed in the zirconia grinding jar. After ball milling, fine powder was obtained, as shown in Figures 1b and 3a.

UVR–vitrimer Powder Mixtures: First, a certain amount of UVR solution was stirred with a horizontal electric mixer (HD2015W, WO-XUAN, China). The vitrimer powder was added at a low stirring speed (60 rpm). The cross stainless-steel impeller of the electric stirrer enabled the powder to be dispersed more evenly in the UVR solution than in the magnetic stirring, without producing sticky aggregates and deposits. In order to make the powder more evenly dispersed, KOS 110 dispersant was added, which accounted for 1% of the total mass of UVR–vitrimer powder mixture solution. Finally, the vitrimer powder was evenly dispersed and mixed in the UVR solution by stirring at a high speed of 600 rpm for 1 h.

Mechanical Test Samples: Dog bone samples used for mechanical testing were printed by DLP. Then, samples were transferred to the oven for heating treatment. Details of the heat treatment (temperature and time, etc.) are described in Section 2.

SEM Observation of Powders and Fracture Surfaces: To observe the size of the vitrimer powders, the microstructures of the fracture surfaces of as-printed and heat-treated samples, morphology observation was conducted on a field-emission SEM (Merlin, Zeiss). The as-printed sample and heat-treated sample were fractured immediately, once the samples were frozen in liquid nitrogen. The vitrimer powders and fracture surfaces were observed with a FE-SEM at an acceleration voltage of 5 kV and electric current of 100 pA.

Particle Size Distribution: The particle size distribution of vitrimer powder after ball milling was measured by a laser granularity apparatus (MASTERSIZER 2000, Malvern Instruments Ltd., UK). Using ethanol as the dispersant, the powder concentration was about 0.0065% vol., and a particle size range from 0.020 to 2000 μm was detected. Each vitrimer powder was tested in six groups and the average value was calculated.

Rheological Test: The viscosity (η) of all mixtures was measured by using a controlled-stress rheometer (DHR2, TA instruments Inc., UK) with an aluminum plate geometry (diameter 25 mm, gap 200 μm). All dynamic rheological data were checked as a function of strain amplitude to ensure that the measurements were performed in the linear domain.

Photorheological Test: The storage modulus and loss modulus of materials were measured on a DHR2 (TA instruments Inc., UK) machine with an aluminum plate geometry (diameter 20 mm, gap 200 μm). First 20 s were detected without light, then 60 s were exposed in 385 nm ultraviolet light with 1, 2, 4, or 8 mW cm^{-2} light intensity, and more 20 s were detected after the end of exposure. Aluminum plate rotated at a speed of 5 rad s^{-1} throughout the 100 s detection process. The intersection of the loss modulus and storage modulus curves is the gel point, and the corresponding time minus 20 s is the gel time.

Dynamic Mechanical Analysis: DMA (Q800 DMA, TA Instruments) was used to characterize the thermomechanical properties of cured mixtures in the tension film mode. Samples with dimensions of 15 mm × 5 mm × 1 mm were tested at a frequency of 1 Hz and an

amplitude of 5 µm. The temperature was first equilibrated at −50 °C for 5 min, and then gradually increased to 100 °C at a heating rate of 2 °C min^{-1}. The glass transition temperatures (T_g) were determined from the peak of the tanδ. Three samples of each mixture with 25 wt% powder (UVR–hard vitrimer mixture, UVR–soft vitrimer mixture, and UVR–UVR powder mixture) were prepared for DMA test.

Uniaxial Tensional Tests: To perform the Young's modulus and ultimate tensile strength of cured mixtures, MTS universal testing machine (MTS Criterion, Model 43.104 Dimensions) was used to carry out tension tests at room temperature. The loading rate was chosen to be a small value (1% per min for all tests) to minimize viscoelastic effects. The size of the middle section (except for the part clamped at both ends) of the samples was approximately 20 mm × 5 mm × 1 mm. For the samples prepared under the same condition, at least three samples were tested, and the average values were reported.

Quasi-Static Compression Test: A quasi-static compression test was carried out at a rate of 0.02 mm s^{-1} with MTS universal testing machine. The octet–truss structure with a compression height of 20 mm was compressed.

3D Printing: The structure was printed layer by layer exposing under UV light by DLP method. The 3D structure was sliced with a target thickness to obtain the cross-section layers as the exposure patterns. The exposure time and ultraviolet light intensity were controlled to obtain an exposure depth equal to the slice thickness. In this paper, the slice thickness was 100 µm, the exposure intensity was 7 mW cm^{-2}, and the exposure time of each layer was 1.5 s. Two self-assembled DLP printers were used in this work (Figure S8, Supporting Information). The downward projection printer based on CEL5500 light engines (wavelength 385 nm, resolution 10.8 microns, projection plane size 36.09 mm × 20.30 mm; Digital Light innovations, Texas Instrument) was used to print structures in this work. The upward projection printer based on HR6500 light engines (wavelength 385 nm, resolution 7 microns, projection plane size 14.66 mm × 8.25 mm; Wintech Digital System Technology Corp.) was used to print planar grids with different widths (Figure 3f–h).

Supporting Information

Supporting Information is available from the Wiley Online Library or from the author.

Acknowledgements

Conflict of Interest

The authors declare no conflict of interest.

Data Availability Statement

The data that support the findings of this study are available in the supplementary material of this article.

[1] M. Capelot, M. M. Unterlass, F. Tournilhac, L. Leibler, *ACS Macro Lett.* **2012**, *1*, 789.

[2] a) B. Krishnakumar, R. P. Sanka, W. H. Binder, V. Parthasarthy, S. Rana, N. Karak, *Chem. Eng. J.* **2020**, *385*, 123820; b) D. Montarnal, M. Capelot, F. Tournilhac, L. Leibler, *Science* **2011**, *334*, 965.

[3] F. Snijkers, R. Pasquino, A. Maffezzoli, *Soft Matter* **2017**, *13*, 258.

[4] a) J. Deng, X. Kuang, R. Liu, W. Ding, A. C. Wang, Y. C. Lai, K. Dong, Z. Wen, Y. Wang, L. Wang, *Adv. Mater.* **2018**, *30*, 1705918; b) D. J. Fortman, J. P. Brutman, C. J. Cramer, M. A. Hillmyer, W. R. Dichtel, *J. Am. Chem. Soc.* **2015**, *137*, 14019; c) Z. Pei, Y. Yang, Q. Chen, E. M. Terentjev, Y. Wei, Y. Ji, *Nat. Mater.* **2014**, *13*, 36; d) Z. Pei, Y. Yang, Q. Chen, Y. Wei, Y. Ji, *Adv. Mater.* **2016**, *28*, 156; e) M. Röttger, T. Domenech, R. van der Weegen, A. Breuillac, R. Nicolaÿ, L. Leibler, *Science* **2017**, *356*, 62; f) B. Zhang, K. Kowsari, A. Serjouei, M. L. Dunn, Q. Ge, *Nat. Commun.* **2018**, *9*, 1831.

[5] a) K. Yu, Q. Shi, M. L. Dunn, T. Wang, H. J. Qi, *Adv. Funct. Mater.* **2016**, *26*, 6098; b) K. Yu, P. Taynton, W. Zhang, M. L. Dunn, H. J. Qi, *RSC Adv.* **2014**, *4*, 10108; c) B. Zhang, C. Yuan, W. Zhang, M. L. Dunn, H. J. Qi, Z. Liu, K. Yu, Q. Ge, *RSC Adv.* **2019**, *9*, 5431; d) H. Li, B. Zhang, K. Yu, C. Yuan, C. Zhou, M. L. Dunn, H. J. Qi, Q. Shi, Q.-H. Wei, J. Liu, *Soft Matter* **2020**, *16*, 1668; e) B. Zhang, H. Li, C. Yuan, M. L. Dunn, H. J. Qi, K. Yu, Q. Shi, Q. Ge, *J. Appl. Polym. Sci.* **2020**, *137*, 49246; f) K. Yu, P. Taynton, W. Zhang, M. L. Dunn, H. J. Qi, *RSC Adv.* **2014**, *4*, 48682; g) Z. Fang, N. Zheng, Q. Zhao, T. Xie, *ACS Appl. Mater. Interfaces* **2017**, *9*, 22077; h) P. Taynton, K. Yu, R. K. Shoemaker, Y. Jin, H. J. Qi, W. Zhang, *Adv. Mater.* **2014**, *26*, 3938.

[6] a) K. Yu, Q. Shi, H. Li, J. Jabour, H. Yang, M. L. Dunn, T. Wang, H. J. Qi, *J. Mech. Phys. Solids* **2016**, *94*, 1; b) Q. Shi, K. Yu, M. L. Dunn, T. Wang, H. J. Qi, *Macromolecules* **2016**, *49*, 5527.

[7] a) K. Yu, H. Yang, B. H. Dao, Q. Shi, C. M. Yakacki, *J. Mech. Phys. Solids* **2017**, *109*, 78; b) X. Kuang, Y. Zhou, Q. Shi, T. Wang, H. J. Qi, *ACS Sustainable Chem. Eng.* **2018**, *6*, 9189.

[8] Q. Shi, K. Yu, X. Kuang, X. Mu, C. K. Dunn, M. L. Dunn, T. Wang, H. J. Qi, *Mater. Horiz.* **2017**, *4*, 598.

[9] Q. Ge, Z. Li, Z. Wang, K. Kowsari, W. Zhang, X. He, J. Zhou, N. X. Fang, *Int. J. Extreme Manuf.* **2020**, *2*, 022004.

[10] a) Y. Yang, E. M. Terentjev, Y. Wei, Y. Ji, *Nat. Commun.* **2018**, *9*, 1906; b) M. O. Saed, A. Gablier, E. M. Terentjev, *Adv. Funct. Mater.* **2020**, *30*, 1906458.

[11] M. M. Obadia, B. P. Mudraboyina, A. Serghei, D. Montarnal, E. Drockenmuller, *J. Am. Chem. Soc.* **2015**, *137*, 6078.

[12] a) W. Wang, J. Sun, B. Guo, X. Chen, K. P. Ananth, J. Bai, *J. Eur. Ceram. Soc.* **2020**, *40*, 682; b) B. Zhang, H. Li, J. Cheng, H. Ye, A. H. Sakhaei, C. Yuan, P. Rao, Y. F. Zhang, Z. Chen, R. Wang, *Adv. Mater.* **2021**, 2101298.

[13] a) K. Yu, Q. Ge, H. J. Qi, *Nat. Commun.* **2014**, *5*, 3066; b) H. J. Qi, T. D. Nguyen, F. Castro, C. M. Yakacki, R. Shandas, *J. Mech. Phys. Solids* **2008**, *56*, 1730; c) C. M. Yakacki, R. Shandas, C. Lanning, B. Rech, A. Eckstein, K. Gall, *Biomater.* **2007**, *28*, 2255.